THE JOURNAL OF THE ACOUSTICAL SOCIETY OF KOREA Vol.22, No.4E 2003. 12. pp. 183~196

Development of Hybrid Method for the Prediction of Internal Flow-induced Noise and Its Application to Throttle Valve Noise in an Automotive Engine

Cheol-Ung Cheong*, Sung-Tae Kim**, Jae-Heon Kim***, Soo-Gab Lee****
*BK21 Post Doc., School of Mechanical and Aerospace Engineering, Seoul National University
**Ph. D. Candidate, School of Mechanical and Aerospace Engineering, Seoul National University
***Technical Venture T.F.T, R&D Division, Hyundai Motor Company
****Professor, School of Mechanical and Aerospace Engineering, Seoul National University
(Received October 29 2003; accepted November 24 2003)

Abstract

General algorithm is developed for the prediction of internal flow-induced noise. This algorithm is based on the integral formula derived by using the General Green Function, Lighthill's acoustic analogy and Curl's extension of Lighthill's. Novel approach of this algorithm is that the integral formula is so arranged as to predict frequency-domain acoustic signal at any location in a duct by using unsteady flow data in space and time, which can be provided by the Computational Fluid Dynamics Techniques. This semi-analytic model is applied to the prediction of internal aerodynamic noise from a throttle valve in an automotive engine. The predicted noise levels from the throttle valve are compared with actual measurements. This illustrative computation shows that the current method permits generalized predictions of flow noise generated by bluff bodies and turbulence in flow ducts.

Keywords: *Internal aerodynamic noise, Valve noise, Generalized green function, Duct acoustics, Dipole & quadrupole source*

I. Introduction

Generation and propagation of flow-induced noise in internal flows have quite different aspects from those in external flows. From a physical standpoint of sound generation and propagation, acoustic waves radiated from noise sources in external flow are affected only by interference of noise sources themselves while those in internal flow are influenced by interference between wall and noise sources in addition to that of noise sources themselves. The interference of wall and noise sources leads to modal solutions to internal acoustic fields. Due to the complexity of aerodynamic noise in internal flow, scarcely any work at all has been reported on the generalized hybrid methods for the prediction of internal aerodynamic noise. There have been only purely numerical and purely theoretical approaches.

For many industrial problems originated from aerodynamic noise, Computational Aeroacousitcs (CAA) technique, reliable and easy to apply, would be of great value to engineers and manufacturers. Recent and spectacular achievements in the understanding of aerodynamic noise generation mechanism are based on the CAA technique using the direct calculation of the acoustic field by solving the unsteady compressible Navier-Stokes equations. Most of them are related to jet noise phenomena, on which the direct numerical simulations[1,2] are carried out, providing

Corresponding author: Soo-Gab Lee (solee@plaza.snu.ac.kr)
School of Mechanical and Aerospace Engineering, Seoul National University, San 56-1, Shilim-Dong Kwanak-Gu Seoul 151-742, Korea

directly an acoustic far field conformable to measurements. However, direct computation of the aerodynamic noise radiated by a subsonic flow remains difficult because of the large computing resources, the expensive cost and physical/numerical issues[3,4] inherent in CAA. It is also evident that the analytic methods[5-10] have some difficulties in serving as general design tools due to their constraint in application arena.

In this paper, semi-analytic model for the prediction of internal aerodynamic noise is developed. This hybrid method is based on the integral formula derived by using inhomogeneous wave equation, General Green Function, Lighthill's acoustic analogy[11] and Curl's extension[12] of Lighthill's. The integral formula is so arranged as to predict the frequency-domain acoustic signal at any location in a duct by using the unsteady flow data in space and time, which can be provided by the computational fluid techniques.

This article contains four sections. In second section, fundamental formulations for the prediction of internal aerodynamic noise are derived. In third section, current method is applied to the flow noise from quick-opening throttle valve in an automotive engine. The numerical results and discussion of flow simulation and noise prediction results by using current hybrid method are described in detail. Final section is devoted to the concluding remarks.

II. Fundamental Formulations

2.1. Equation for the Sound Field

Coordinates moving with uniform mean flow are chosen with origin on one edge of the pipe, y_1 being coordinate in the axial direction, and y_2 and y_3 in the cross-sectional plane. The problem of sound generated by a flow in a duct can be treated by replacing the solid obstacle by a distribution of dipole sources and the turbulence by a distribution of quadrupole sources, respectively. Then, the equation governing the sound field in the duct is Lighthill's form and Curl's extension from Lighthill's as follows.

$$\left\{\nabla^2-\frac{1}{c^2}\frac{\partial^2}{\partial\tau^2}\right\}p(y_k,t)=\left(\frac{\partial}{\partial y_i}\right)[f_i(y_k,t)]-\left(\frac{\partial}{\partial y_i}\right)\left[\frac{\partial T_{ij}}{\partial y_j}\right] \tag{1}$$

where p is the pressure, τ is time, c is the velocity of sound, f_i is force per unit volume and T_{ij} is Lighthill's turbulence stress tensor. T_{ij} denotes the expression $(p - c^2\rho)\,\delta_{ij} + \rho u_i u_j$, where δ_{ij} is the Kronecker delta and u_i is the particle velocity in the i-direction relative to the mean flow. Upon assuming that the density fluctuation are negligible within the moving fluid, the turbulence stress tensor is approximately equal to $\rho u_i u_j$. It is also assumed that the modeled source terms in right-hand side of (1) act over a limited region of the duct.

In addition to satisfying Eq. (1), the solution must satisfy appropriate boundary conditions, which are that all waves are outgoing at infinity, and that the normal velocity vanishes at the walls. At the hard walls, the normal component of particle velocity must vanish and the boundary condition on the pressure at the duct walls is

$$\frac{\partial p}{\partial n}=0 \tag{2}$$

where n is the normal to the wall. Eq. (1) can be solved by means of a Green's function $G(\mathbf{x},t \mid \mathbf{y},\tau)$ defined as the solution of

$$\nabla^2 G-\frac{1}{c^2}\frac{\partial^2 G}{\partial\tau^2}=\delta(\mathbf{x}-\mathbf{y})\delta(t-\tau) \tag{3}$$

with $\frac{\partial G}{\partial n}=0$ on the boundaries.

The Fourier transform of G with respect to time, written $g(\mathbf{x},\mathbf{y}\mid\omega)$ satisfies the equation

$$\nabla^2 g - k^2 g = \delta(\mathbf{x}-\mathbf{y}) \tag{4}$$

and is related to G by the inverse transform

$$G(x,t\mid y,\tau)=\frac{1}{2\pi}\int_{-\infty}^{\infty} g(x,y\mid\omega)\exp\{-i\omega(t-\tau)\}d\omega \tag{5}$$

The Green's function is expressed as a sum of the normal modes of oscillation. First, consider the eigenfunction Ψ_{mn} satisfying the following 2-D Helmholz equation and the boundary condition.

$$\left(\frac{\partial^2}{\partial y_2^2}+\frac{\partial^2}{\partial y_3^2}\right)\Psi_{mn}+\kappa_{mn}^2\Psi_{mn}=0 \quad with \quad \frac{\partial\Psi}{\partial n} = 0 \ on \ the \ boundaries \tag{6}$$

The eigenfunction Ψ_{mn} are orthonormal; that is, if A is the cross-section of a duct,

$$\int_A \Psi_{mn}\Psi_{m'n'}dy_2dy_3=\begin{cases} 0 \ if \ m\neq m' \ or \ n\neq n' \\ \Gamma_{mn} \ if \ m=m' \ and \ n=n \end{cases} \tag{7}$$

Then, the solution of (4) can be assumed to be the sum of the product of the eigenfunction and the function of the y_1 as

$$g_\omega=\sum_{m,n=0}^{\infty} f_{mn}(y_1)\Psi_{mn}(y_2,y_3) \tag{8}$$

This form of solution automatically satisfies the wall boundary condition due to Eq. (6). The insertion of (8) into (4) and using Eq. (5) lead to

$$\sum_{m,n=0}^{\infty}\left(\frac{d^2}{dy_1^2}+k_0^2-\kappa_{mn}^2\right)f_{mn}\Psi_{mn}=\delta(\mathbf{x}-\mathbf{y}) \tag{9}$$

Multiplying both side of (9) by the conjugate of the eigenfunction, integrating the resultant equation on the area perpendicular to the duct axis, and using the relation of (7), ordinary equation for f_{mn} can be obtained as follows.

$$\left(\frac{d^2}{dy_1^2}+k^2-\kappa_{mn}^2\right)f_{mn}=\frac{\Psi_{mn}^*(x_2,x_3)}{\Gamma_{mn}}\delta(\mathbf{x}-\mathbf{y}) \tag{10}$$

The solution of (10), going to infinity, can be expressed as

$$f_{mn}=\frac{i\Psi_{mn}^*(x_2,x_3)}{2k_{mn}\Gamma_{mn}}\exp\{ik_{mn}|x_1-y_1|\} \tag{11}$$

where $k_{mn}=\sqrt{k^2-\kappa_{mn}^2}$. By using Eq. (5), Green Function in time-domain can be expressed as

$$G(\mathbf{x},t\,|\,\mathbf{y},\tau)= \frac{i}{4\pi}\sum_{m,n=0}^{\infty}\frac{\Psi_{m,n}(y_2,y_3)\Psi_{m,n}^*(x_2,x_3)}{\Gamma_{m,n}}\int_{-\infty}^{\infty}\frac{\exp\{ik_{mn}|x_1-y_1|\}}{k_{m,n}} \exp\{-i\omega(t-\tau)\}d\omega \tag{12}$$

By using the above equation, time-domain acoustic pressure from internal flow can be expressed as

$$p(\mathbf{x},t)=c^2\rho(\mathbf{x},t)=\int_v\int_\beta G(\mathbf{x},t\,|\,\mathbf{y},\tau)\left\{\frac{\partial f_i(\mathbf{y},\tau)}{\partial y_i}-\frac{\partial^2 T_{ij}(\mathbf{y},\tau)}{\partial y_i\partial y_j}\right\}dyd\tau$$

where the volume integral is over all space and the time integral ranges from -∞ to ∞. The Green function chosen is an exact form, and with boundary conditions specified, ensures that the solution involves no surface integrals. Thus,

$$p(\mathbf{x},t)=c^2\rho(\mathbf{x},t)=\frac{i}{4\pi}\sum_{m,n=0}^{\infty}\frac{\Psi_{m,n}^*(x_2,x_3)}{\Gamma_{m,n}} \int dy\int_{-\infty}^{\infty}d\tau\int_{-\infty}^{\infty}d\omega\Psi_{m,n}(y_2,y_3)\frac{\exp\{ik_{mn}|x_1-y_1|-i\omega(t-\tau)\}}{k_{m,n}}\left\{\frac{\partial f_i(\mathbf{y},\tau)}{\partial y_i}-\frac{\partial^2 T_{ij}(\mathbf{y},\tau)}{\partial y_i\partial y_j}\right\} \tag{13}$$

The term k_{mn}, defined by (11), denotes the wave number in the axial direction. For propagating wave motion this must be real, which it is above the cut off frequency which is denoted by $\omega_{mn}=ck_{mn}$. For frequency less than the cut-off frequency, k^2_{mn} is negative and the pressure in that mode decays exponentially away from the source. Similar form of integral equation has been used in previous theoretical studies[5-6,9].

2.2. Rearrangement for Semi-analytic Algorithm

In this section, Eq. (13) is rearranged in order to develop the general hybrid algorithm, by which the internal aerodynamic noise signal can be predicted. Rearrangement is carried out such that frequency-domain noise signal at certain position in a duct can be computed by using unsteady flow data in time and space, which are provided by using the Computational Fluid Dynamics techniques.

First, consider the inverse Fourier transform of Eq. (13) on the time t at position $\mathbf{x}$, and then ω component of pressure p at poison $\mathbf{x}$ can be described as follows.

$$p(\mathbf{x},\omega)=\frac{i}{2}\sum_{m,n=0}^{\infty}\frac{\Psi_{m,n}^*(x_2,x_3)}{\Gamma_{m,n}} \int_v dy\int_{-\infty}^{\infty}d\tau\Psi_{m,n}(y_2,y_3)\frac{\exp\{ik_{mn}|x_1-y_1|+i\omega\tau)\}}{k_{m,n}}\left\{\frac{\partial f_i(\mathbf{y},\tau)}{\partial y_i}-\frac{\partial^2 T_{ij}(\mathbf{y},\tau)}{\partial y_i\partial y_j}\right\} \tag{14}$$

In order to combine above equation with given flow data in space and time, Eq. (14) is rewritten as follows.

$$p(\mathbf{x},\omega)=\frac{i}{2}\sum_{m,n=0}^{\infty}\frac{\Psi^{*}_{m,n}(x_2,x_3)\exp\{ik_{mn}x_1\}}{\Gamma_{m,n}}\{\mathbf{D}_{mn}(\omega)+\mathbf{Q}_{mn}(\omega)\}$$

where

$$\mathbf{D}_{mn}(\omega)=\int_{-\infty}^{\infty}\int_{V}\Psi_{m,n}(y_2,y_3)\frac{\exp\{-ik_{mn}y_1+i\omega\tau)\}}{k_{m,n}}\left\{\frac{\partial f_i(\mathbf{y},\tau)}{\partial y_i}\right\}dvd\tau$$

$$\mathbf{Q}_{mn}(\omega)=-\int_{-\infty}^{\infty}\int_{V}\Psi_{m,n}(y_2,y_3)\frac{\exp\{-ik_{mn}y_1+i\omega\tau)\}}{k_{m,n}}\left\{\frac{\partial^2 T_{ij}(\mathbf{y},\tau)}{\partial y_i\partial y_j}\right\}dvd\tau \tag{15}$$

Here, $\mathbf{D}_{mn}$ denotes the ω component of noise from dipole sources and $\mathbf{Q}_{mn}$ does from quadrupole sources. By applying the divergence theorem to (15) with integral space enough to cover the whole field at the boundary of which the sources disappear, Eq. (15) can be rewritten as follows.

$$\mathbf{D}_{mn}(\omega)=-\frac{1}{k_{m,n}}\int_{-\infty}^{\infty}\int_{V}f_i(\mathbf{y},\tau)\frac{\partial}{\partial y_i}\{\Psi_{m,n}(y_2,y_3)\exp\{-ik_{mn}y_1+i\omega\tau)\}\}dvd\tau$$

$$\mathbf{Q}_{mn}(\omega)=-\frac{1}{k_{m,n}}\int_{-\infty}^{\infty}\int_{V}T_{ij}(\mathbf{y},\tau)\frac{\partial}{\partial y_i\partial y_j}\{\Psi_{m,n}(y_2,y_3)\exp\{-ik_{mn}y_1+i\omega\tau)\}\}dvd\tau \tag{16}$$

Unsteady data provided by flow simulations can be used to calculate the terms of f_i and T_{ij} of (16). For a cylindrical duct, the eigenfunction of (6) can be expressed as

$$\Psi_{m,n}=J_m(\kappa_{m,n}r)e^{-im\theta} \tag{17}$$

where $r=\sqrt{y_2^2+y_3^2}$, $\theta=\tan^{-1}(y_2/y_3)$. Here, J_m is m-th Bessel function κ_{mn} and is n-th root of the following equation.

$$J'_m(\kappa_{m,n}r_d)\equiv\left.\frac{dJ_m(x)}{dx}\right|_{x=\kappa_{m,n}r_d}=0$$

From Eq. (7), the following equation can be obtained.

$$\Gamma_{mn}=\pi\left(r_d^2-\frac{m^2}{\kappa_{mn}^2}\right)J_m^2(\kappa_{mn}r_d)$$

The insertion of (17) into (16) leads to

$$\mathbf{D}_{mn}(\omega)=\frac{1}{k_{m,n}}\int_{-\infty}^{\infty}\int_{V}f_i(\mathbf{y},\tau)\frac{\partial}{\partial y_i}\left\{J_m(\kappa_{m,n}r)e^{-i(k_{mn}y_1+m\theta)}\right\}\exp\{i\omega\tau\}dvd\tau$$

$$\mathbf{Q}_{mn}(\omega)=\frac{1}{k_{m,n}}\int_{-\infty}^{\infty}\int_{V}T_{ij}(\mathbf{y},\tau)\frac{\partial}{\partial y_i\partial y_j}\left\{J_m(\kappa_{m,n}r)e^{-i(k_{mn}y_1+m\theta)}\right\}\exp\{i\omega\tau\}dvd\tau \tag{18}$$

It is convenient to convert the rectangular coordinates into the cylindrical coordinates in Eq. (18) because the Green Function of (17) is expressed as the cylindrical coordinates.

III. Application to the Intake Noise from a Throttle Valve in an Automotive Engine

Semi-analytic model, described in previous section, is applied to the throttle valve noise problem. Figure 1 shows behavior of throttle angle and flow-induced noise, as measured when the throttle is opened quickly. For this measurement, the airflow is suctioned through the outlet of manifold at the volume flow rate corresponding to that of 2000 cc engine at operating condition of 1500 rpm and the throttle angle was changed from fully closed (5 Deg.) to wide-open (90 Deg.) in 0.227 second. This measurement shows that the strong noise signal is generated when the throttle is opened through angles 20 Deg. to 50 Deg.

3.1. Analysis of Airflow Upon Quick Opening of Throttle

Market-available analysis tool, STAR-CD is used for the flow analysis. The reasons for using the commercial software for the flow analysis instead of an in-house code are two-fold. The first is to show the capability of the developed algorithm to be combined with the commercial software, which is more convenient tool for engineers in the practical fields. The second is to avoid the severe code validation for the saving of time. The utilized algorithm in STAR-CD is as follows: QUICK scheme[13] is used for spatial discretization, fully implicit scheme[14] for time discretization, and the solution algorithm is based on the PISO algorithm[15]. To numerically analyze a three-dimensional flow, the flow fields must be represented by a calculation mesh. The flow field configuration changes as the throttle continues opening. The calculation area is divided into the duct section and the spherical section. The spherical section contains the baffle cells modeling the throttle valve and allows for the rotation of the baffle cell, i.e., the throttle valve. Fig. 2 shows the calculation meshes where the entire spherical section is rotated about the

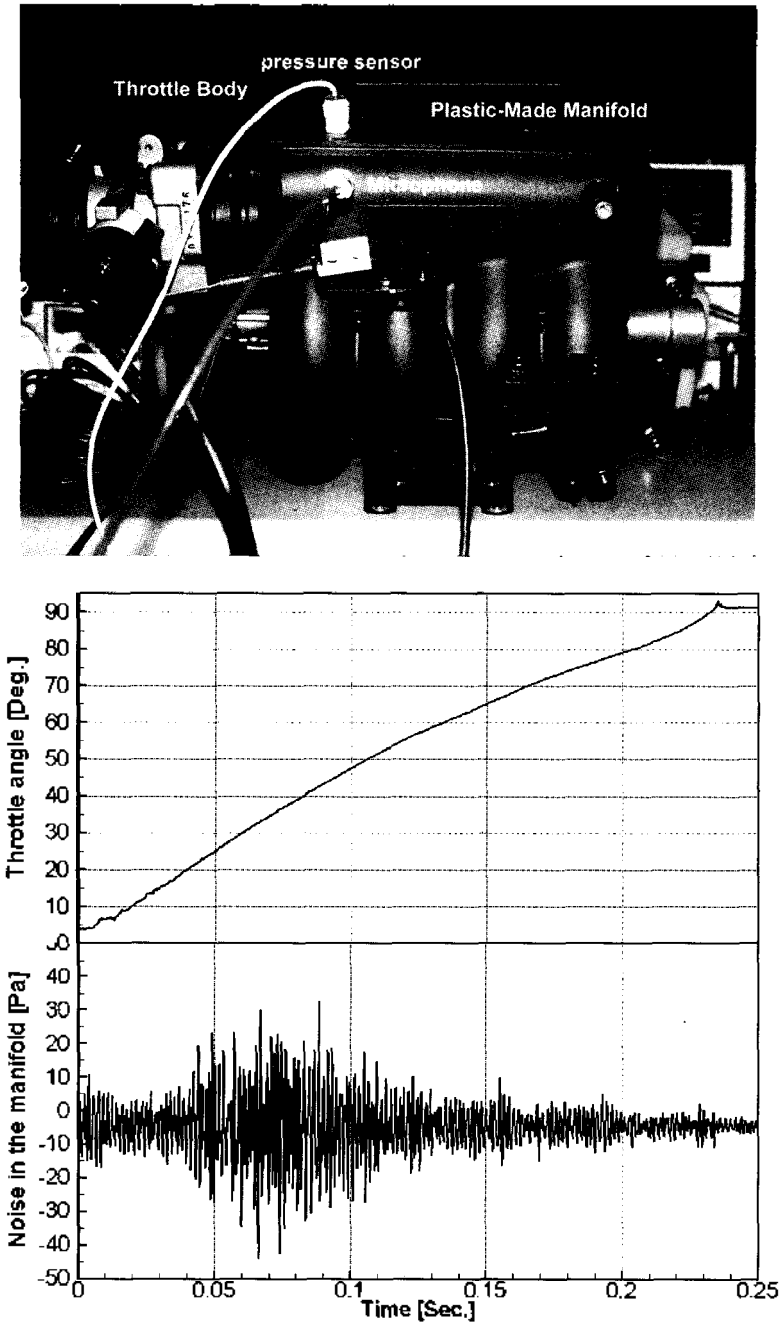

Figure 1. Throttle body and manifold for actual measurement, behavior of throttle angle and flow-induced noise from the quick-opening throttle valve.

throttle axis and the applied boundary conditions. This made it comparatively easy to prepare a calculation mesh for each throttle valve angle, which enabled numerical analysis for every airflow configuration change. Moving boundary between the duct and spherical meshes is accommodated with the arbitrary sliding interface method [16]. Making use of symmetric geometry of the concerned problem, only a half section of the throttle is analyzed for the saving of calculation time. The Mesh for the simulation contains 26355 nodes and 22820 hexahedral elements.

The throttle opening time, from fully closed position to fully open position, is 0.227 second, which is set to meet the experimental condition. The fluid is assumed to be a compressible viscous flow with the properties of air. To reproduce the throttle conditions as much as possible, the measured value of pressure at points upstream and

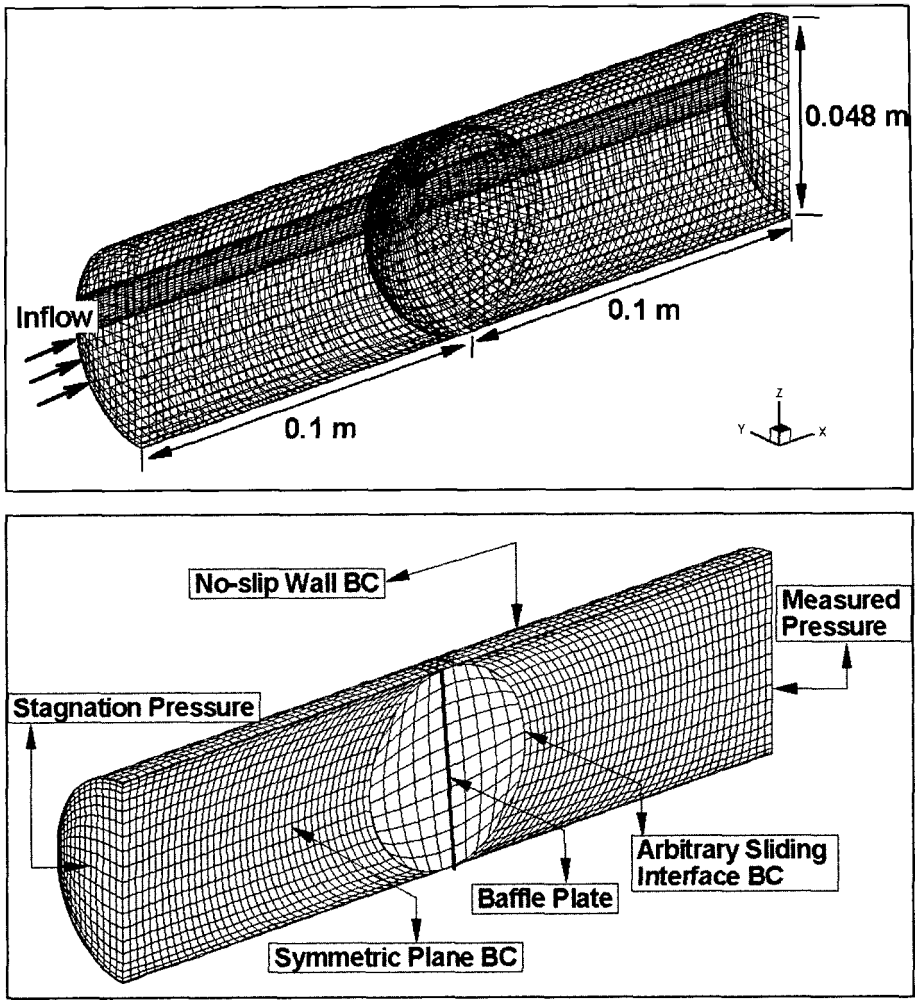

Figure 2. Mesh for calculation and dimensions for the throttle valve and the conduit and applied boundary conditions.

downstream from the throttle is used as inflow and outflow boundary conditions. The pressure at inlet plane is kept almost constantly at atmospheric pressure, while the pressure on the exit side increases steadily from low pressure to nearly atmospheric pressure during the quick opening behavior of the throttle. Fig. 3 shows the measured pressure at the exit side.

In the following, the airflow characteristics are analyzed at three throttle open angles; 20, 30 and 40 degree. In Fig. 4 are shown the distribution of velocity vectors for airflow at a longitudinal cross section passing through the duct axis with airflow from left to right when the throttle is opened to 20 degree. The flow speed vector diagram shows very fast airflow in the upper part of the throttle. This airflow is divided into an eddy current that flows back toward the throttle valve, and a flow that whirls into

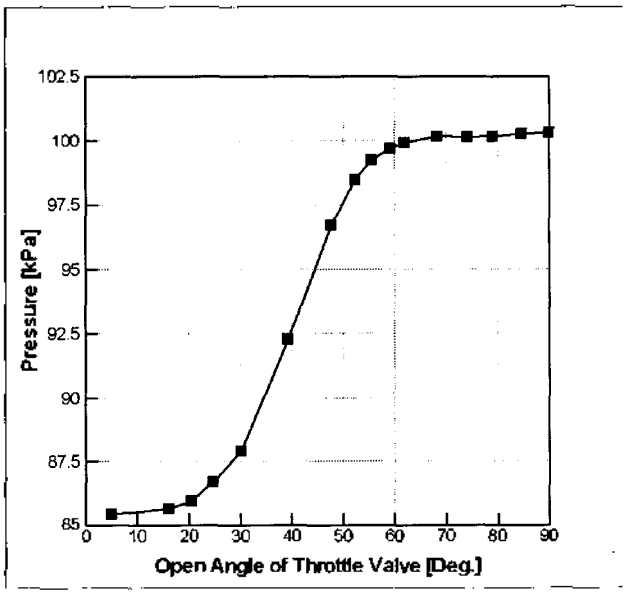

Figure 3. Measured pressure history at the outlet of the duct for the numerical simulation.

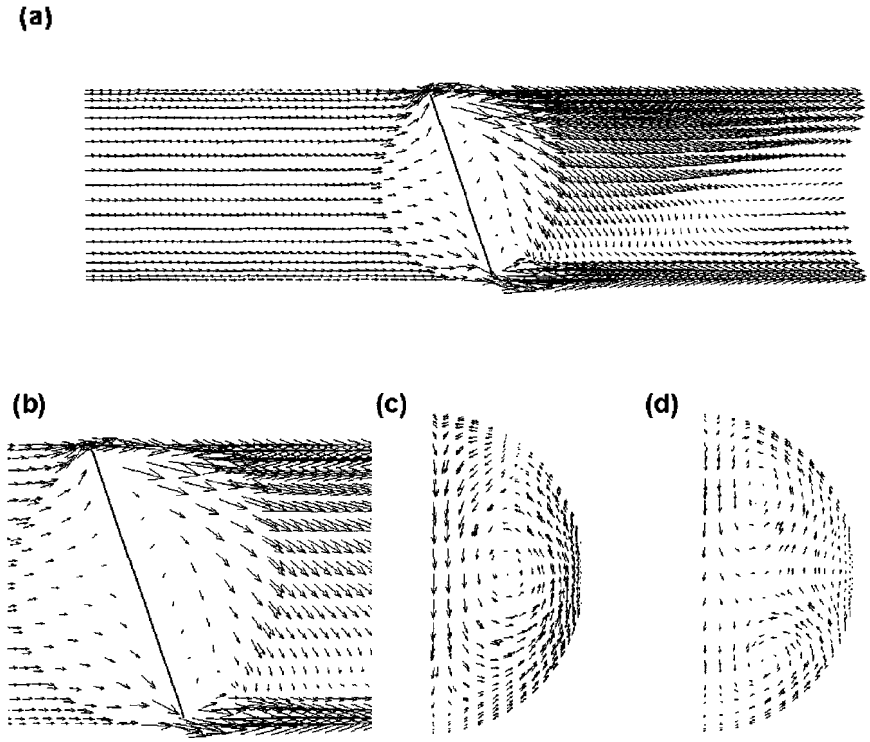

Figure 4. Velocity distribution of airflow when the throttle valve is opened to *20* degree (Maximum Vel. = 141.3 m/s): (a) at the plane $y = 0$, (b) zoomed plot, (c) at the plane $x = 0.3$ and (d) at the plane $x = 0.6$.

the lower part of the throttle. Observation of the airflow along a cross section perpendicular to the duct axis shows a flow in the central area of the duct that travels from the upper part to the lower part of the throttle. As a result, it can be found that the anti-symmetric vortex lines are formed in the downstream after the airflow passes through the throttle valve. Generation of the anti-symmetric vortex lines is thought to be most important phenomena in that these vortex lines feed the turbulence and, as a result, works as main energy source for aerodynamic noise. Fig. 5 presents the contours of the pressure and the turbulence kinetic energy. The pressure contour diagram shows that, at relatively small open angle mimicking the initial stage of throttle valve opening, the pressure in the area downstream is low, indicating that the airflow does not reach the exit of the conduit. Turbulence kinetic energy K, calculated by the k-ε model, has a large value over a wide area downstream from the throttle valve and the maximum region is located on the lower part of the duct in the symmetric plane.

In Fig. 6 are shown the distribution of velocity vector when the throttle is opened to 30 degree. The flow speed vector diagram shows that a very fast airflow passes through the upper and lower parts of the throttle. The vector diagram of a cross section perpendicular to the duct axis shows also the eddy current, observed in the previous case, in the pattern; the stream starts from the upper part of the throttle, and passes through the central area of the duct to flow into the lower part of the throttle and then leave the lower part of the throttle and flows into the upper part of the throttle, along the inner wall of the duct. At an area 30 to 60 mm downstream from the throttle, air flows from both the upper and lower parts of the throttle mix and merge. It can be found that the merging of the two flows and the resultant eddy is most intense in this case. Fig. 7 presents the contours of the pressure and the turbulence kinetic energy at open angle of 30 degree. In comparison with that of 20 degree, the pressure increases gradually in the area downstream from the throttle valve. There is a large turbulent flow area still.

In Fig. 8 are shown the distribution of velocity vector for the 40 degree of valve open angle. There is no big

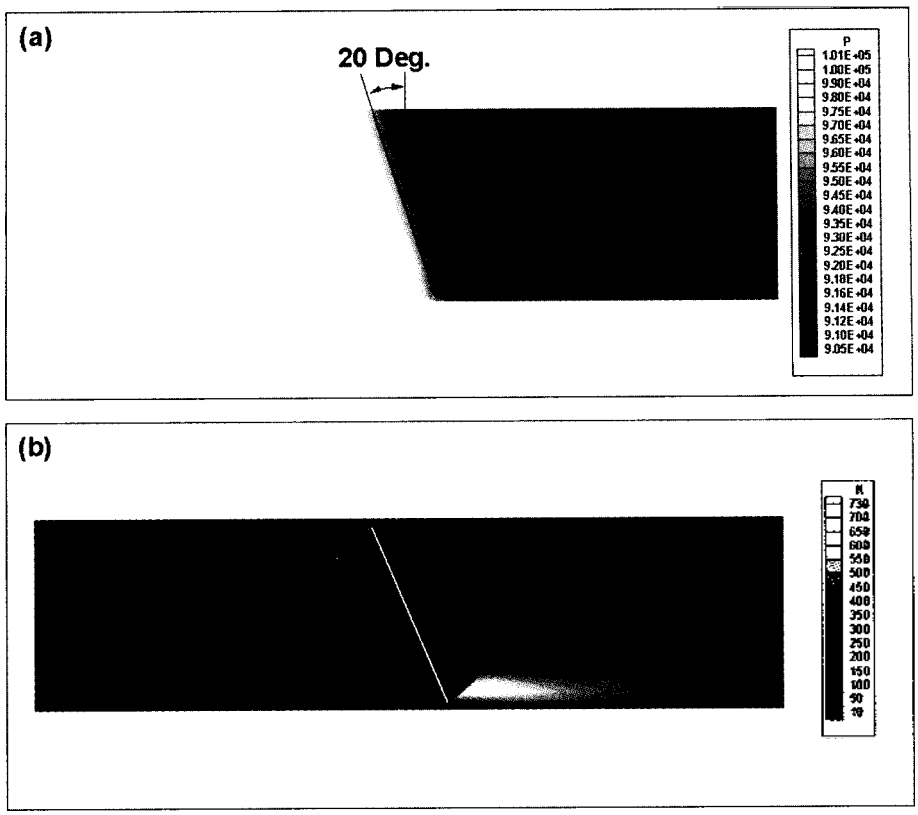

Figure 5. Distributions of (a) pressure and (b) turbulence kinetic energy at the symmetric plane $y = 0$ at the open angle of *20* degree.

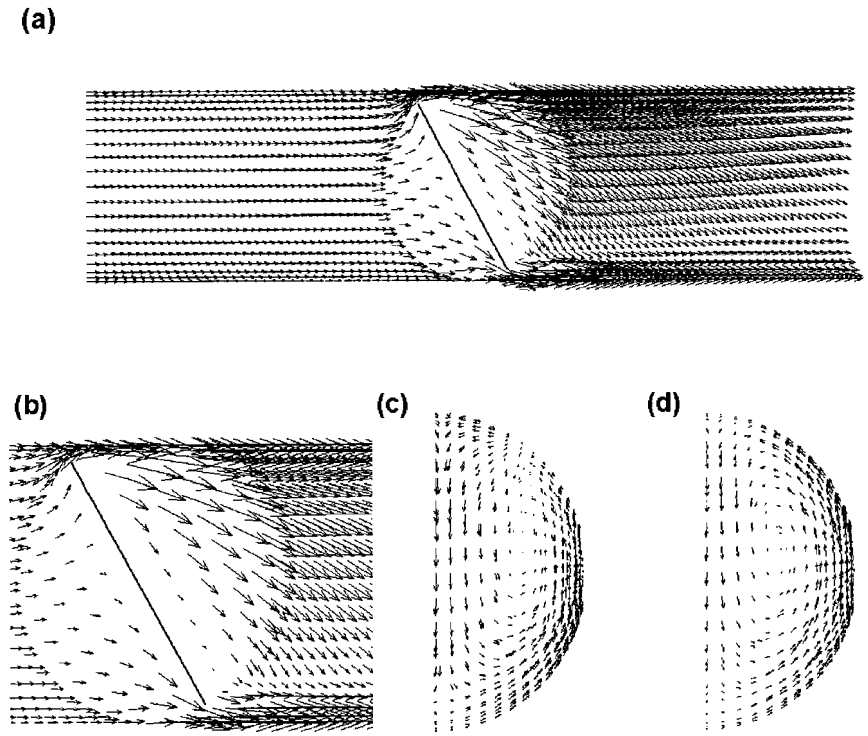

Figure 6. Velocity distribution of airflow when the throttle valve is opened to *30* degree (Maximum Vel. = 142.5 m/s):(a) at the plane $y = 0$, (b) zoomed plot, (c) at the plane $x = 0.3$ and (d) at the plane $x = 0.6$.

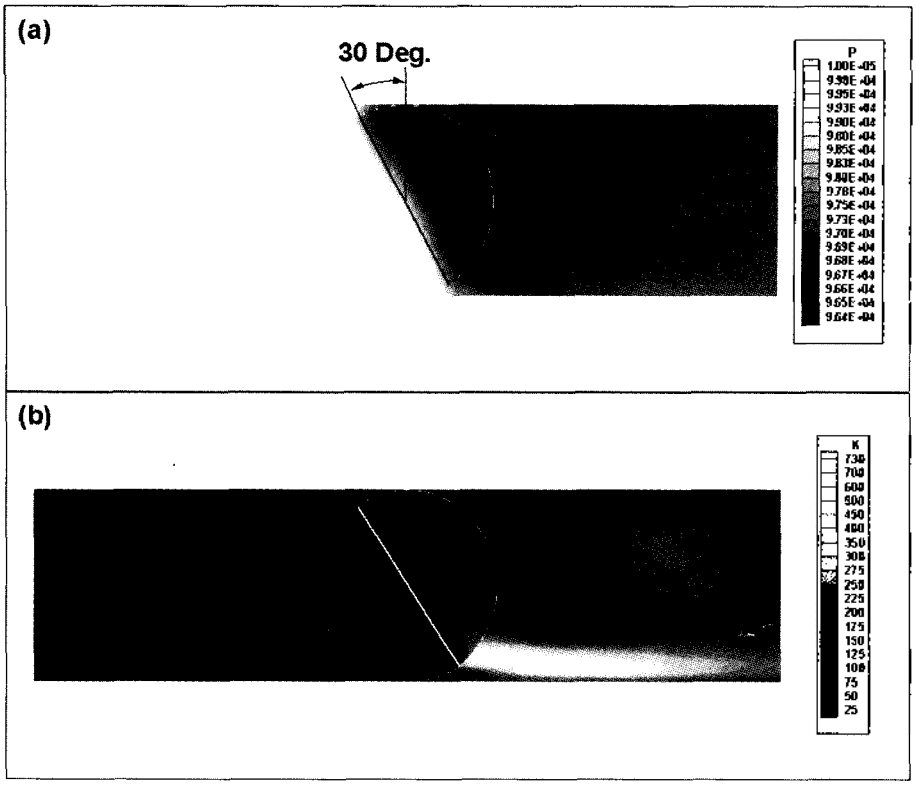

Figure 7. Distributions of (a) pressure and (b) turbulence kinetic energy at the symmetric plane $y = 0$ at the open angle of *30* degree.

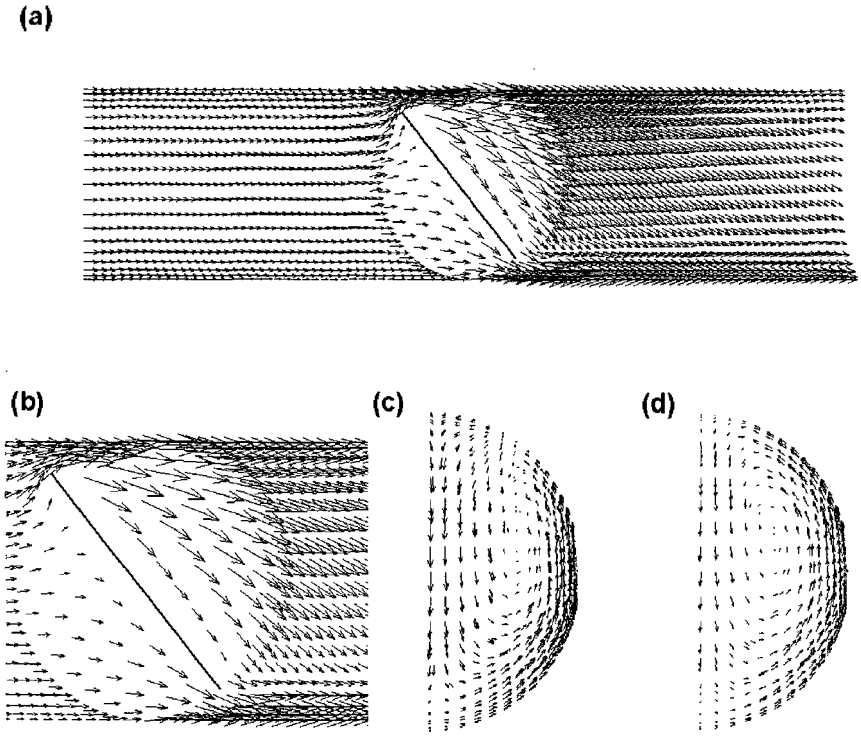

Figure 8. Velocity distribution of airflow when the throttle valve is opened to *40* degree (Maximum Vel. = 112.9 m/s): (a) at the plane $y = 0$, (b) zoomed plot, (c) at the plane $x = 0.3$ and (d) at the plane $x = 0.6$.

difference in the velocity distribution between the present case and the previous two cases. However, it is distinguished from the previous cases in that airflow around the throttle valve in this case goes parallel to the wall of the throttle, and thus the reverse flow from the lower part of the throttle disappears. This flow patterns are due to, as the open area is more increased, the maximum speed of airflow around the throttle is more decreased and thus the airflow passes more smoothly through the splits between the throttle and the inner-surface of the conduit. Fig. 9 presents the contours of the pressure and the turbulence kinetic energy at open angle of 40 degree. The maximum of the turbulence kinetic energy is decreased into 30% lower value than those of previous two cases.

In the range of the open angles over 50 degree, the velocities of airflows passing through the upper and lower parts of the throttle are suddenly decreased when compared with those of previous cases. Although the eddy resulting form the whirling airflow has still existed, the magnitude of the vortex are also rapidly constricted. As a result the magnitude of the turbulence kinetic energy has also decreased very much compared with previous three cases.

3.2. Prediction of Internal Aerodynamic Noise

In this section, the internal aerodynamic noise from the quick-opening throttle valve is predicted by combining the developed semi-analytic model and the previously calculated flow data. It is found that the components below 4150 Hz are cut-off frequencies and only (0,1) mode, i.e., plane wave is propagated. The time step in previous flow simulation is 0.0002 second and the Nyquist frequency is 2000 Hz. Thus, in present noise prediction with previously calculated flow data, only plane mode is valid.

Prediction is carried out based on Eqs. (15), (16) and (18). From a physical standpoint, computation of Eqs. (15), (16), and (18) may be considered to be filtering processes that dipole sources of unsteady pressure on the surface of the throttle and quadrupole sources of turbulent

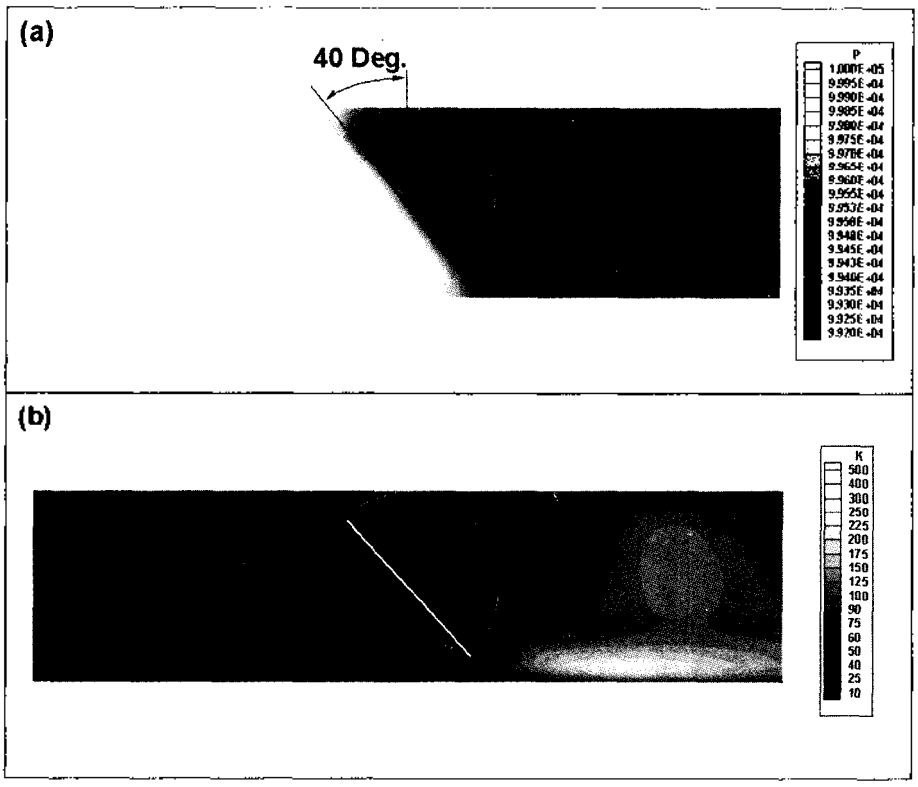

Figure 9. Distributions of (a) pressure and (b) turbulence kinetic energy at the symmetric plane $y = 0$ at the open angle of 40 degree.

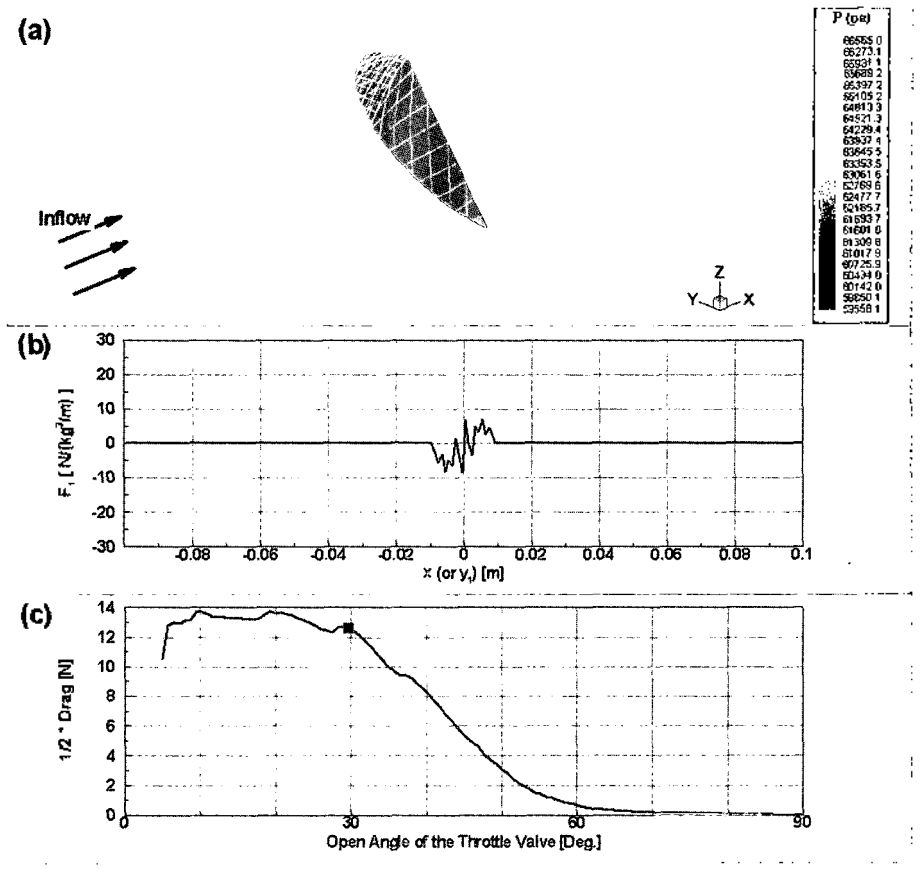

Figure 10. The dipole sources of airflow when the throttle valve is opened to 30 degree: (a) pressure distribution on the surface of the throttle valve, (b) variation of F_l along the direction of flow stream and (c) the drag of the throttle valve.

velocities in flow are filtered with the Green function determined by the geometry of cross-section of a duct through the time and space integration. Figure 10 presents the pressure distribution on the surface of the throttle valve, F_l variation along the direction of flow stream and the drag of the throttle valve at the open angle 30-degree (marked with the filled rectangle) with whole variation of the drag during the full opening behavior. The distribution of F_l is more elongated along the flow stream direction compared with that at the smaller open angle. The distribution of F_l in time and space is utilized for the calculation of the dipole-originated, plane-mode noise signal using Eq. (18). The drag of the throttle at open angle 30 degree is on the verge of declination after passing through maximum region of the drag. In the range of open angle over 50 degree, the distribution of F_l is more widely expanded than the previous cases. The drag of the throttle is also rapidly decreased.

Fig. 11 presents the variation of turbulence kinetic energy over whole computation domain, the distribution of T_l along the flow-stream direction, and space-integrated values of T_{ll} over whole computation domain at the open angle 30-degree (marked with the filled rectangle) with whole variation of T_{ll} during the entire opening behavior. Here, T_{ll} is utilized to calculate the quadrupole- originated, plane-mode noise signal. From this figure, it is found that most of downstream region behind the throttle is filled with the strong turbulence having the high turbulent kinetic energy and T_l has also very high value over the range from $y_l = -0.01\ m$ to $y_l = 0.05\ m$. The total integrated value of T_{ll} is also located at the maximum region in whole variation of T_{ll}. At the stage of the open angle over 50 degree, as the passage area between the throttle valve and the inner surface of the conduit is more increased, the air streams passes more smoothly through the passage area and thus turbulence kinetic energy is also

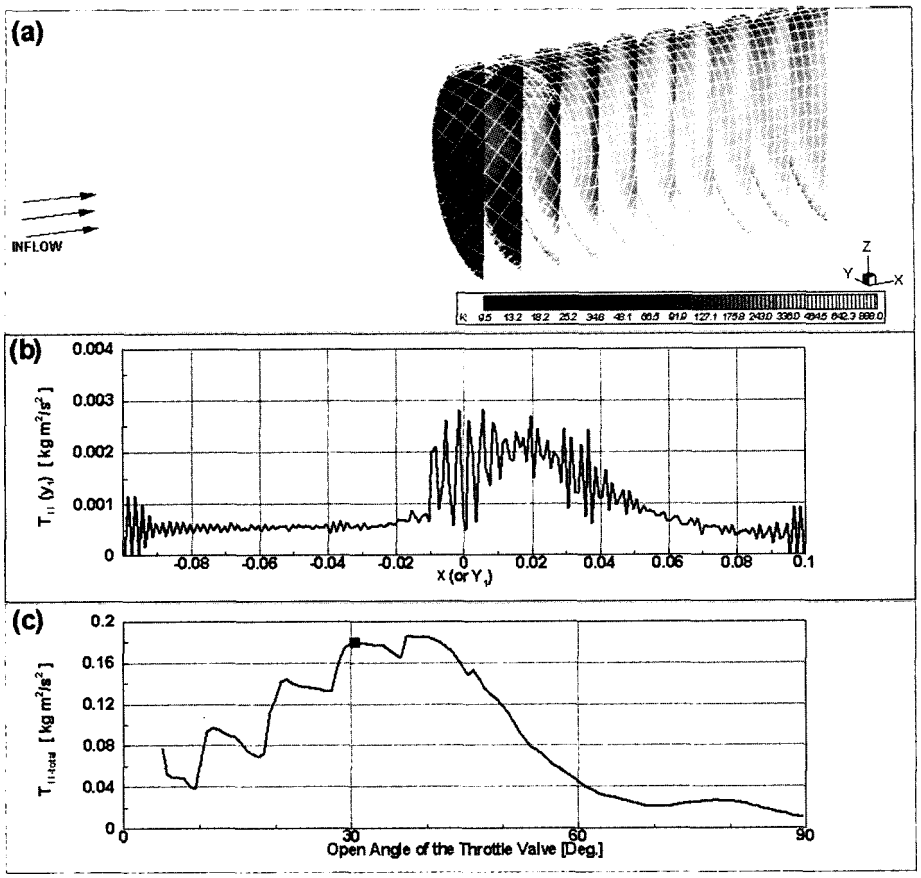

Figure 11. The quadrupole sources of airflow when the throttle valve is opened to 30 degree: (a) The variation of turbulence kinetic energy over whole computation domain, (b) the distribution of T_{ij} along the flow-stream direction, and space-integrated values of T_{ij} over whole computation domain.

steeply decreased. The maximum value of total turbulence kinetic energy in the range over 60 degree open angle is approximately five-times lower than the maximum value in the whole range.

Fig. 12a shows the calculated dipole- and quadrupole-originated noise levels, with measured data in the frequency band from 88 Hz to 1760 Hz. In this frequency range, only the plane mode is cut-on mode. It is found from this figure that the noise level from the dipole sources is bigger than that from the quadrupole sources, and thus noise generation mechanism from the quick opening throttle seems to be dipole-originated phenomena. It is also found that, although the discrepancy of prediction results of dipole noise from the measured values is approximately 8[dB] at each frequency, the decreasing trend of the predicted noise level according to the frequencies agrees well with that of the testing results. For all frequency range, the predicted noise level is bigger than that of the measurement, i.e., the simulation results tend to be an over-prediction. This is because the cross-sectional area of the pipe suddenly changes as the airstreams flow from the duct containing the throttle valve to the manifold where the measurement is executed. From the theoretical analysis [17], the relation between the strength, I, of the incident harmonic pressure wave and the strength, T, of the transmitted wave is described as follows.

$$T = \frac{2A_1}{A_1 + A_2} I \tag{19}$$

where A_1 and A_2 are the areas of incident duct and transmitted duct, respectively. In this case, A_1 is the area of the conduit containing the throttle valve, $\pi \times 0.024^2[m^2]$ and A_2 is that of the manifold, $0.0796 \times 0.0735[m^2]$. Insertion of these areas into (19) leads to the transmission loss -6.5 dB. Fig. 12b shows the sound pressure levels of the raw prediction, corrected prediction by using the transmission

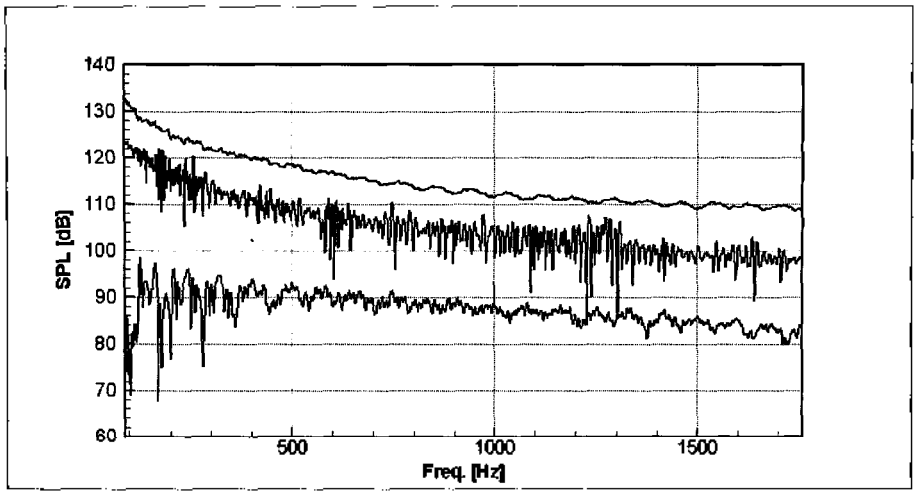

(a)

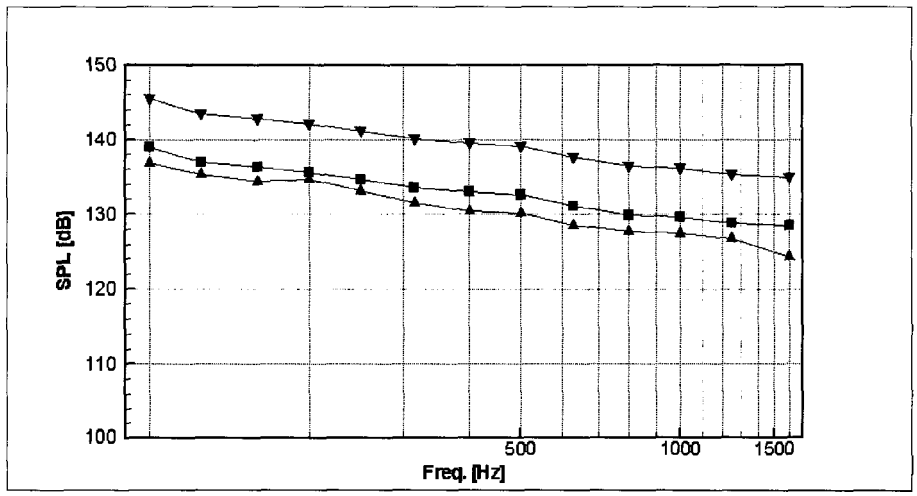

(b)

Figure 12. Comparison of sound pressure levels: (a) at Δf = 1 (Upper: Predicted results by using the dipole source, middle: Measured Data, and Lower: Predicted results by using the quadrupole source (b) at one-third octave band frequencies. (▼: Prediction result, ■: Corrected prediction result by using the transmission loss, and ▲: measured data)

loss, and the measured data on one-third octave band frequencies. The predicted noise level after the correction agrees quite well with the measured level. It can still be confirmed that the proposed methodology for predicting the internal aerodynamic noise is a reliable approach and it can provide us a powerful and efficient method for further noise reduction and control of the internal flow-induced noise.

IV. Concluding Remarks

The hybrid method is developed for the prediction of internal flow-induced noise from obstacles, i.e. dipole sources and turbulent velocities, i.e. quadrupole sources. This method is based on the integral formula derived by using the General Green Function, Lighthill's acoustic analogy and Curl's extension of Lighthill's. Novel approach of this algorithm is that the integral formula is so arranged as to predict the frequency-domain acoustic signal at any locations in a duct by using the unsteady flow data in space and time, which can be provided by the Computational Fluid Dynamics techniques. This semi-analytic model is applied to the prediction of the internal aerodynamic noise from a quick-opening throttle valve in an automotive engine. The predicted noise level of the throttle valve shows similar decreasing trend according to the frequencies with the measurements. The prediction

results corrected with the transmission loss shows good agreements with the measurement than the raw prediction data. This illustrative numerical application shows that the current method permits generalized predictions of flow noise generated by bluff bodies and turbulence in flow ducts.

Acknowledgment

This work is supported by the International Cooperation Research Program of the Ministry of Science & Technology.

References

1. B. E. Mitchell, S. K. Lele, and P. Moin, "Direct computation of mach wave radiation in an axisymmetric supersonic jet," *AIAA J.*, **35**, 1574-1580, 1997.
2. J. B. Freund, "Acoustic sources in a turbulent jet: a direct numerical simulation study," *CEAS/AIAA Paper, 98-1858, 1999.*
3. C. K. W. Tam, "Computational aeroacoustics: issues and methods," *AIAA J.*, **33**, 1788-1790, 1995.
4. S. K. Lele, "Computational aeroacoustics: a review," AIAA 97-0018, 1997.
5. P. E. Doak, "Excitation, transmission and radiation of sound from source distributions in hard-walled ducts of finite length (I): The effects of duct cross-section geometry and source distribution space-time," *Journal of Sound and Vibration*, **31**, 1-72, 1973.
6. H. G. Davies and J. E. Ffowcs Williams, "Aerodynamic sound generation in a pipe," *Journal of Fluid Mechanics*, **32**, 765-778, 1968.
7. C. G. Gordon, "Spoiler-generated flow noise (I): The experiment," *Journal of the Acoustical Society of America*, **43**, 1041-1048, 1968.
8. C. G. Gordon, "Spoiler-generated flow noise (I): results," *Journal of the Acoustical Society of America*, **45**, 214-223, 1969.
9. P. A. Nelson and C. L. Morfey, "Aerodynamic sound production in low speed flow ducts," *Journal of Sound and Vibration*, **79**, 263-289, 1981.
10. D. J. Oldham and A. U. Ukopoho, "A pressure-based technique for predicting regenerated noise levels in ventilation systems," *Journal of Sound and Vibration*, **140** (2), 263-289, 1990.
11. M. J. Lighthill, "On sound generated aerodynamically - I. general theory," *Proceedings of the Royal Society Series A.*, **211**, 564-587, 1952.
12. N. Curle, "The influence of solid boundaries upon aerodynamic sound," *Proceedings of the Royal Society Series A.*, **231**, 505-514, 1955.
13. B. P. Leonard, "A stable and accurate convective modeling procedure based on quadratic upstream interpolation," *Comput. Method Appl. Mech. Engng.*, **19**, 56-98, 1979.
14. R. D. Richtmeyer, and K. W. Morton, *Difference Methods for Initial-Value Problems*, 2nd Edition, Wiley-Interscience, New York, 1967.
15. R. I. Issa, "Solution of the implicitly discretised fluid flow equations by operator-splitting," *J. Comp. Phys.*, **62**, 4065, 1986.
16. I. Demirdzic, and M. Peric, "Space conservation law in finite volume calculations of fluid flow," *Int. J. Numer. Methods in Fluids*, **8**, 1037-1050, 1988.
17. A. P. Dowling, and J. E. Ffowcs Williams, *Sound and Sources of Sound*, Ellis Horwood Limited, 1983.

[Profile]

• Cheol-Ung Cheong

1997, B.S. in Aerospace Eng. Seoul National University.
1999, M.S. in Aerospace Eng. Seoul National University.
2003, Ph.D. in Aerospace Eng. Seoul National University.
2003~Present: BK21 Postdoctoral Research Associate, Seoul National University.
※ Major Research Topics: Computational Aeroacoustics, Trubofan Noise, Duct Acoustics, Jet Noise, Shear Layer Noise.

• Sung-Tae Kim

2001, B.S. in Aerospace Eng. Seoul National University.
2001~Present: Ph. D. Candidate in School of Mechanical and Aerospace Engineering.
※ Major Research Topics: Computational Aeroacoustics, Tyre Noise.

• Jae-Heon Kim

1992, B.S. in Aerospace Eng. Seoul National University.
1994, M.S. in Aerospace Eng. Seoul National University.
1998, Ph.D. in Aerospace Eng. Seoul National University.
1998~Present: Senior Researcher, Technical Venture T.F.T, R&D Division, Hyundai Motor Company.
※ Major Research Topics: Acoustic and Performance of Power Train in an Automotive.

• Soo-Gab Lee

1983, B.S. in Aerospace Eng. Seoul National University.
1985, M.S. in Aerospace Eng. Seoul National University.
1992, Ph.D. in Aerospace Eng. Stanford University.
1992~1995: Nasa Ames, Senior Researcher.
1996~Present: Professor, School of Mechanical and Aerospace Engineering
※ Major Research Topics: Helicopter Aerodynamics and Acoustics, Rotating Machinery Noise (Rotor, Fan, Propeller, Compressor, Turbine), High Speed Vehicle Noise (Aircraft, High Speed Train, Automobiles), Active Noise Control, Duct-related Acoustics, Termoacoustics (Combustion Instability and Noise), Computational Aeroacoustics, Sound quality.